Photon amplification in a two-photon lossless micromaser

H. Moya-Cessa,* P. L. Knight, and A. Rosenhouse-Dantsker†
Optics Section, The Blackett Laboratory, Imperial College, London SW7 2BZ, England
(Received 11 March 1994)

We investigate the interaction of atoms through two-photon resonant transitions, with quantized cavity radiation, in the framework of a lossless micromaser theory. Taking advantage of the fact that the atomic inversion is quasiregular in time in this model, with quite precise revivals, we find a very strong amplification of the average photon number. At the two-photon revival time, the atom leaves the cavity in an almost pure state. This leads to an essentially noise-free process that results in a shift of two photons of the initial photon distribution each time an atom passes through the cavity, while the width of the photon distribution remains constant. This leads to strongly sub-Poissonian field statistics.

PACS number(s): 42.50.Dv, 42.52.+x

I. INTRODUCTION

There has been a great deal of interest in the past few years in the generation of sub-Poissonian light fields and especially in producing the limiting case of a pure number state. There are several schemes that have been proposed to produce number states [1–5], by using micromasers in which a quantized field in a high-Q cavity is successively pumped by a stream of Rydberg atoms arranged such that only one atom at most is present at any instant in the cavity. Experiments on one-photon micromasers have demonstrated the importance of describing the cavity field in a fully-quantum-mechanical way: an observation of the revival (see Rempe, Walther, and Klein [1]) of Rabi oscillations relates to the discreteness of the cavity field and an observation of sub-Poissonian statistics [1] demonstrates how atom-field dynamics can reduce the quantum noise of the field below the coherent-field values.

The theory of the two-photon micromaser has been developed in some detail [6] and experiments have been carried out [3]. In this micromaser context, Garraway *et al.* [4] have proposed a simple scheme that allows the generation and detection of nonclassical states of light, by conditional measurements. Their method is based on the condition that the atom is measured in the excited state after interaction with the cavity field. This results in an overlap of peaks in the phase space of the state of the field conditioned by the atomic measurement, whose interference results in the production of Fock states. In the present paper we study the interaction of atoms and radiation through two-photon resonant transitions in a lossless cavity. We consider a special case of flight time, (i.e., of atom-field interaction time) and show that number states can be generated (in fact, an almost noiseless amplification of the photon statistics may be achieved). This special time we consider is the two-photon revival time [7], $t_R=\pi/\lambda$, for which atoms exit the cavity so that the field and atoms are left almost in a pure state (see Fig. 1).

The paper is organized as follows: In Sec. II we investigate the dynamics of the two-photon Jaynes-Cummings model which underpins idealizations of micromasers, paying particular attention to the atomic inversion (for which, and for some fields, we find very accurate approximate expressions) and the photon distribution (PD). In Sec. III we generalize the results of Sec. II, allowing atoms to leave and enter the cavity (one at a time), finding the expression for the field density matrix after k atoms have passed through it. This enables us to compute several variables of interest. We then investigate photon distributions for various initial field statistics, which allow us to compute the sub-Poissonian factor for the fields, as well as the average photon number in the cavity. Finally, Sec. IV is devoted to conclusions.

II. TWO-PHOTON DYNAMICS

In this section we study the atomic behavior when light interacts with matter in a two-photon resonant transition. We consider the two-photon Hamiltonian (we consider units such that $\hbar=1$)

$$\hat{H}=(\omega_0+\chi\hat{a}^\dagger\hat{a})\sigma_3+\omega\hat{a}^\dagger\hat{a}+\lambda[\sigma_+\hat{a}^2+(\hat{a}^\dagger)^2\sigma_-]\,, \qquad (2.1)$$

where λ is the coupling constant; $\hat{a}$ and $\hat{a}^\dagger$ are the annihilation and creation operators for the field mode, respectively; and $\sigma_+=|e\rangle\langle g|$ and $\sigma_-=|g\rangle\langle e|$, where $|e\rangle$ ($|g\rangle$) means excited (ground) atomic state, are the Pauli spin-flip operators for the two-photon transitions. We consider the intermediate state to be so far from resonance that it can be adiabatically eliminated to give an effective two-photon coupling of the above form as well as a Stark shift, leading to an intensity-dependent transition frequency [8]. The Stark-shift coefficient is denoted as χ, the unperturbed atomic frequency by ω_0, and the

*Present address: Instituto Nacional de Astrofísica, Optica y Electrónica, Laboratorio de Fotónica, Apartado Postal 51 y 216, 72000 Puebla, Puebla, Mexico.
†Present address: Department of Chemistry, Bar-Ilan University, Ramat Gan 52900, Israel.

cavity-field frequency by ω. Knight and Shore [9] have investigated the validity of this adiabatic elimination procedure for a single atom evolution.

We employ the method of Stenholm [10] using the interaction picture Hamiltonian

$$\hat{H}_I=(\Delta+\chi\hat{a}^\dagger\hat{a})\sigma_3+\lambda[\sigma_+\hat{a}^2+(\hat{a}^\dagger)^2\sigma_-] .$$

to obtain the time-evolution operator

$$\hat{U}^\dagger(t)=\exp(i\hat{H}_I t/\hbar)$$

($\Delta=\omega_0-2\omega$), expressing it in the atomic basis (see [7])

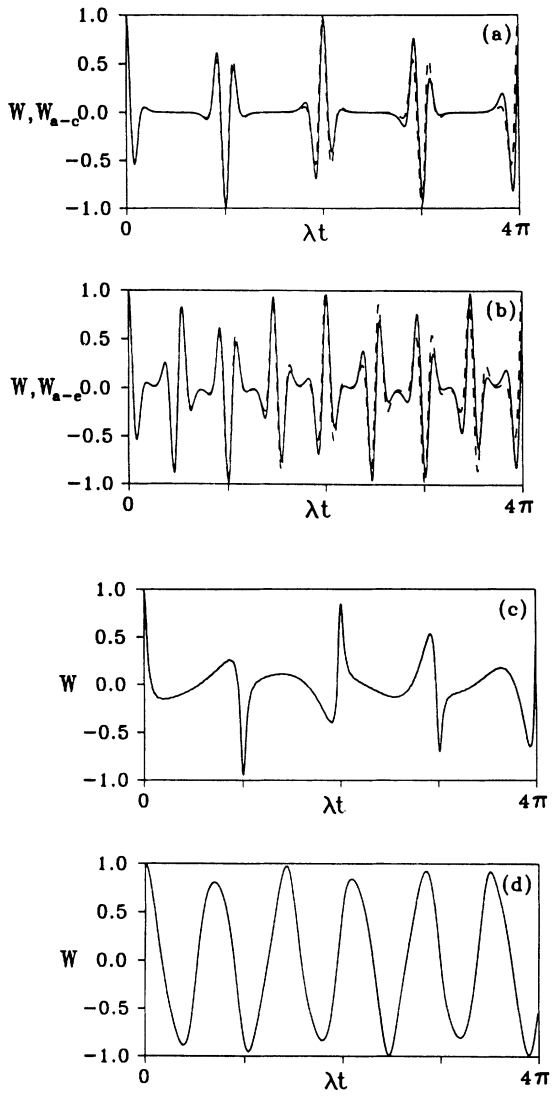

FIG. 1. Two-photon atomic inversion as a function of scaled time λt with the atom initially in its excited state, $\Delta=0$ and $\chi=0$: (a) Field in an initial coherent state with $\bar{n}=4$, exact expression (solid line), i.e., W as given in Eq. (2.5); and approximate expression (dashed line), i.e., $W_{a\text{-}c}$ as given in Eq. (2.7). (b) Initial even coherent state with $\bar{n}=4$, exact expression (solid line), i.e., W as given in Eq. (2.5); and approximate expression (dashed line), i.e., $W_{a\text{-}e}$ as given in Eq. (2.9). (c) Initial thermal field with $\bar{n}=4$. (d) Initial squeezed vacuum field, $r=\frac{1}{2}$ i.e., $\bar{n}=0.27$.

$$\hat{U}^\dagger(t)=\exp(-i\chi t/2)\begin{bmatrix}\hat{C}_n & i\hat{S}_n^\dagger\\ i\hat{S}_n & \hat{C}_{n-2}\end{bmatrix} , \tag{2.2}$$

where we have defined

$$\hat{C}_n=\cos(\hat{\delta}_n t)+i\frac{\hat{\Gamma}_n}{\hat{\delta}_n}\sin(\hat{\delta}_n t) , \tag{2.3a}$$

$$\hat{S}_n=\lambda\hat{b}^\dagger\frac{\sin(\hat{\delta}_n t)}{\hat{\delta}_n} , \tag{2.3b}$$

$$\hat{\delta}_n^2=\hat{\Gamma}_n^2+\lambda^2\hat{b}\hat{b}^\dagger=\hat{\Gamma}_n^2+\lambda^2(\hat{n}+1)(\hat{n}+2) , \tag{2.3c}$$

and

$$\hat{\Gamma}_n=\frac{\Delta+\chi(\hat{n}+1)}{2} , \tag{2.3d}$$

with $\hat{b}=\hat{a}^2$. We can now write the expression for the total density matrix, given by

$$\rho(t)=\hat{U}(t)\rho(0)\hat{U}^\dagger(t) ,$$

with

$$\rho(0)=|e\rangle\langle e|\otimes\rho_F(0) ,$$

so that

$$\rho(t)=\begin{bmatrix}\hat{C}_n\rho_F(0)\hat{C}_n^\dagger & i\hat{C}_n\rho_F(0)\hat{S}_n^\dagger\\ -iS_n\rho_F(0)\hat{C}_n^\dagger & \hat{S}_n\rho_F(0)\hat{S}_n^\dagger\end{bmatrix} . \tag{2.4}$$

From Eq. (2.4) it is easy to find the atomic inversion W from the trace, $W=\mathrm{tr}[\rho(t)\sigma_3]$,

$$W(t)=\sum_{n=0}P_n\left[\frac{\Gamma_n^2}{\delta_n^2}+\frac{(n+1)(n+2)}{\delta_n^2}\cos[2\lambda t\delta_n]\right] , \tag{2.5}$$

where P_n is the initial PD and $\mathcal{O}_n=\langle n|\hat{\mathcal{O}}_n|n\rangle$ (with $\mathcal{O}=\delta,\Gamma$).

If we assume the initial field to be in a coherent state $|\alpha\rangle$, where

$$|\alpha\rangle=\exp(-|\alpha|^2)\sum_{n=0}^{\infty}\frac{\alpha^n}{\sqrt{n!}}|n\rangle , \tag{2.6}$$

and consider the on-resonance case ($\Delta=0$) $\chi=0$ and the approximation

$$[(n+1)(n+2)]^{1/2}\cong n+\tfrac{3}{2} , \tag{2.7}$$

by expressing the cosine in Eq. (2.5) in terms of exponentials and performing the summation, we can obtain an approximate expression for $W(t)$ as

$$W_{a\text{-}c}(t)=\exp[-|\alpha|^2(1-\cos2\lambda t)]\cos[3\lambda t+|\alpha|^2\sin2\lambda t] . \tag{2.8}$$

If, instead of a coherent state as initial field, we have a superposition of coherent states, e.g., an even coherent state [11] (or a Schrödinger cat state)

$$|\psi\rangle_{ev}=\frac{1}{N^{1/2}}[|\alpha\rangle+|-\alpha\rangle]\ , \tag{2.9}$$

where

$$N=2+2\exp(-2|\alpha|^2)$$

is the normalization constant, the corresponding approximation of Eq. (2.5) is

$$W_{a\text{-}e}=\frac{4}{N}\exp(-|\alpha|^2)\{\cos 3\lambda t\cos[|\alpha|^2\sin 2\lambda t]\times\cosh[|\alpha|^2\cos 2\lambda t]-\sin 3\lambda t\sin[|\alpha|^2\sin 2\lambda t]\times\sinh[|\alpha|^2\cos 2\lambda t]\}\ . \tag{2.10}$$

In Figs. 1(a) and 1(b) we plot the atomic inversion, as a function of the scaled time (λt), for the coherent and even coherent states as initial fields, respectively. We use both an exact expression (2.5) (solid lines) and approximate expressions (2.8) and (2.10) (dashed lines). Even for modest photon numbers (here $|\alpha|^2=4$), we see very close agreement between the exact and approximate expressions for the inversion. For the atomic inversion driven by the even coherent states as an initial field, a new revival at $t_0=t_R/2=\pi/2\lambda$ appears, as occurs in the usual Jaynes-Cummings model for one-photon transitions [12]. In Figs. 1(c) and 1(d) we also plot atomic inversions for two other different fields (with different mean photon numbers): a thermal state and a squeezed vacuum [13]. We note that for all these four fields the atomic inversion closely approaches the ground-state value of -1 at t_R. This means that the atom and the field almost decorrelate at this time [7], with the atom returning to the ground (pure) state and giving all the energy it carried to the field. At t_R, the Rabi oscillations have revived although the initial condition is reobtained only at $2t_R$. This is simply understood in phase space: the initial coherent-state quasiprobability bifurcates [14] and recombines at t_R but only at $2t_R$ do the components recombine at the initial value. In a two-photon transition this results in a sign change which is visible in Fig. 1. The revival behavior is very sensitive to Stark shifts for one-photon transition [9], but in our case (two-photon transition) the approach of W to -1 at $t\cong t_R$ is still pronounced (see Fig. 2). In Fig. 2(a) we show the atomic inversion on resonance, for a field intensity $|\alpha|^2=4$, but with a Stark-shift parameter of $\frac{1}{2}$ (in units of λ), which produces a mean detuning of 2. We note an upwards shift of the atomic inversion from the minima produced when there is no Stark detuning. However, the atom is still close to the ground state around $t\cong t_R$. We can compensate for this shift by introducing a detuning that balances the mean detuning produced by the Stark shift. This is seen in Fig. 2(b), which shows a partial restoration of the deep minima in the inversion.

In Sec. III we will investigate how the purity of the field evolves when atoms are allowed to leave and enter the cavity in a micromaser. We next calculate the photon-number distribution at a given time. In order to do that, we compute the field density matrix $\rho_F(t)=\mathrm{tr}_A[\rho(t)]$, where tr_A means trace over the atomic basis

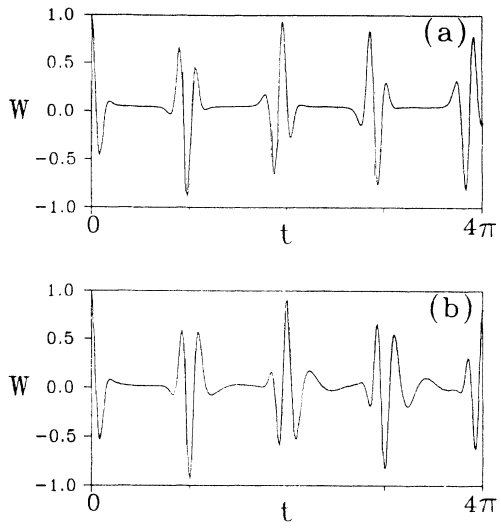

FIG. 2. Two-photon inversion as a function of time; the atom is initially in the excited state, and the field in a coherent state $|\alpha|^2=4$. We have set $\lambda=1$. (a) The Stark-shift parameter is $\chi=\frac{1}{2}$ (in units of λ) and $\Delta=0$. (b) The Stark-shift parameter is $\chi=\frac{1}{2}$ and we choose a value of detuning that balances the effective detuning produced by the Stark-shift parameter, i.e., $\Delta=2$.

$$\rho_F(t)=\hat{C}_n\rho_F(0)\hat{C}_n^{\dagger}+\hat{S}_n\rho_F(0)\hat{S}_n^{\dagger}\ . \tag{2.11}$$

We then write the photon distribution as

$$P_n(t)=|A_n|^2P_n(0)+B_n^2P_{n-2}(0)\ , \tag{2.12}$$

where

$$A_n=\langle n|\hat{C}_n|n\rangle \tag{2.13}$$

and

$$B_n=\frac{\lambda^2n(n-1)}{\delta_n^2}\sin[\delta_n t]\ . \tag{2.14}$$

In Sec. III we will generalize Eq. (2.12), to the case when we have atoms entering and leaving the cavity, successively with no more than one atom at any time present in the cavity.

III. MICROMASER GENERALIZATION

In this section we find an expression for the photon distribution after k atoms have passed through the cavity and, from this, we compute the average number of photons in the cavity and the sub-Poissonian factor κ (equal to Q_M+1, where Q_M is the Mandel Q parameter [15]) as a function of the number of atoms k that have passed through the cavity. We show that strong sub-Poissonian fields can be generated, as well as fields with increased photon number. We then calculate the field density matrix (after k atoms have passed through the cavity) in order to analyze the dynamics in phase space, i.e., by using

the Q function [14]. In addition, we use the field density matrix to compute the purity parameter [16]

$$\zeta=1-\mathrm{tr}_F\{[\rho_F^{(k)}(t_I)]^2\}$$

(where tr_F means trace over the field basis). We also investigate the case of different interaction times.

A. Photon distributions

Equation (2.12) describing the time-dependent photon distribution holds for any initial photon statistics. We evaluate it for an interaction time t_I, at which the atom leaves the cavity having modified the field. We employ this new field as the initial condition for the next atomic interaction. In other words, we have now an initial field, with initial statistics given by

$$P_n^{(2)}(0)=P_n^{(1)}(t_I)=P_n(t_I)\ ,$$

to interact with the next atom. Because we are in the interaction picture, the field statistics does not change while there is no atom in the cavity (remember we are not considering losses). By repeating the process k times, we obtain the photon distribution after k atoms (all initially excited) have passed through the cavity, each interacting for a time t_I [see Eq. (2.12)]:

$$P_n^{(k)}(t_I)=A_n^2P_n^{(k-1)}(t_I)+B_n^2P_{n-2}^{(k-1)}(t_I)\ . \tag{3.1}$$

We can now compute the average number of photons in the cavity, after k atoms have interacted, as

$$\bar{n}^{(k)}(t_I)=\sum_{n=0} nP_n^{(k)}(t_I)\ . \tag{3.2}$$

By using Eqs. (3.1) and (3.2), we find the sub-Poissonian factor κ as

$$\kappa(t_I)=\frac{\langle[\Delta n^{(k)}(t_I)]^2\rangle}{\bar{n}^{(k)}(t_I)}\ . \tag{3.3}$$

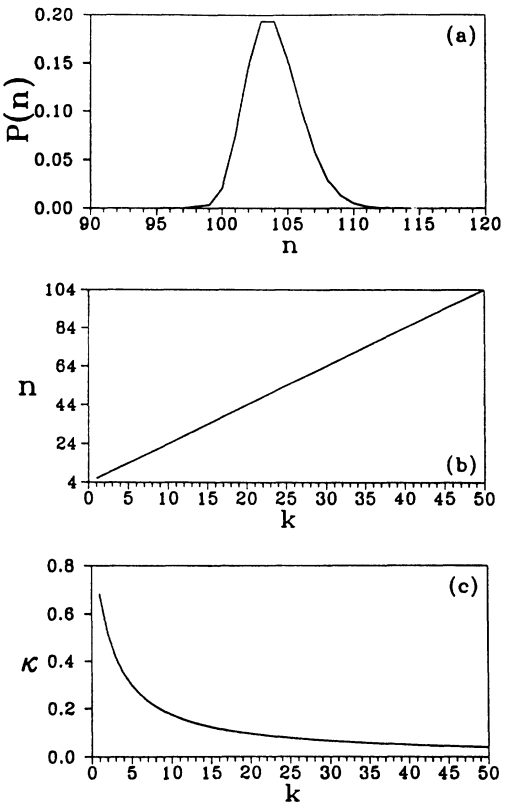

FIG. 3. (a) Photon distribution $P(n)$ as a function of n after 50 atoms have passed through the cavity; (b) average photon number versus the number of atoms that have passed through the cavity; k; and (c) the sub-Poissonian factor, κ vs k. The field is initially in a coherent state $|\alpha|^2=4$; the atoms enter the cavity in their excited state. Each atom interacts for a time $t=t_R$ with the cavity field. We set $\chi=\Delta=0$.

In Fig. 3(a), we plot the PD for an initial coherent state, $|\alpha|^2=4$, $\Delta=0$, and $\chi=0$, after 50 atoms have interacted with the field, with $t_I=t_R=\pi/\lambda$. We note that the PD has basically the same shape, but has been shifted by 100 photons, twice the number of two-photon emitters. Instead of the photon-number distribution being centered on the initial value of 4, it is centered on 104, but the distribution width remains approximately the initial one. In Fig. 3(b), we show the average number of photons, as a function of the number of atoms that have passed through the cavity. Each atom, because of the choice of the interaction time (see Fig. 1), leaves two photons in the cavity (all its energy). We note that for a large number of photons, this follows analytically from Eq. (2.12). If we apply the approximation (2.7), which can also be written $[n(n-1)]^{1/2}\cong n-\frac{1}{2}$, it follows that for interaction times equal to the revival time $t_I=t_R=\pi/\lambda$, Eqs. (2.13) and (2.14) become ($\Delta=\chi=0$) $A_n\cong 0$ and $B_n\cong(-1)^{n+1}$, respectively. Thus, Eq. (2.12) for the photon distribution becomes

$$P_n(t_R)=P_{n-2}(0)\ .$$

We note linear amplification of the photon number. This has previously been noted by Cao Chang-qi and Ding Xiao-hong [17]. When we take into account both the constant width and photon amplification, we expect to see an increasingly sub-Poissonian factor κ as the number of atoms passing through the cavity increases. This is shown in Fig. 2(c). We can see that strongly sub-Poissonian fields can be generated and, as we increase k, κ goes slowly to zero as the fractional width approaches the limiting case of $\kappa=0$, the limiting case of a number state.

In Figs. 4 and 5, we have evaluated the same variables as in Fig. 3, but for an initial thermal state ($\bar{n}=4$) and for a squeezed vacuum with a squeezing parameter $r=\frac{1}{2}$, respectively. We note basically the same behavior in the three figures. However, we can see that the atomic pumping does not result in a pure shift in the PD, because we note the existence of small satellites on the left of the PD's. In latter sections we present analytic results using an asymptotic expansion which neglects these effects.

In Figs. 6 and 7 we look at how the effects shown in Figs. 3–5 are changed when we consider a nonzero Stark parameter. Figure 6 shows the same variables as in Fig. 3

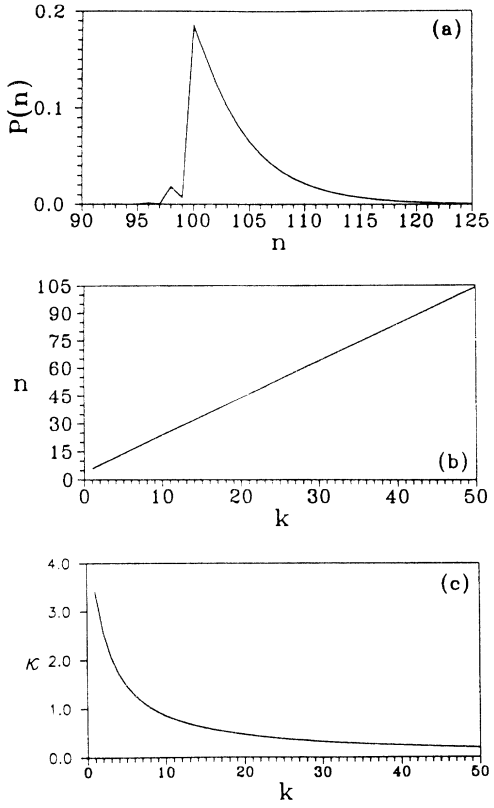

FIG. 4. Same as Fig. 3, but the initial field is described by a thermal distribution, with $\bar{n}=4$.

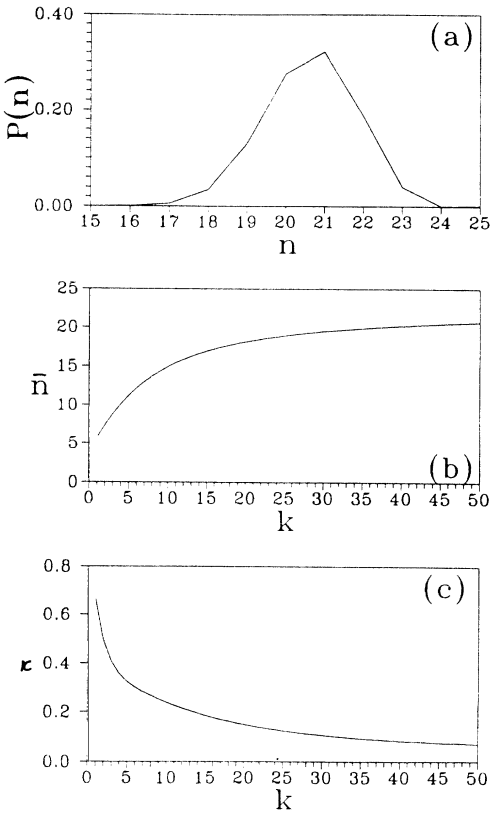

FIG. 6. Same as Fig. 3, but $\chi=\frac{1}{2}$ (in units of λ).

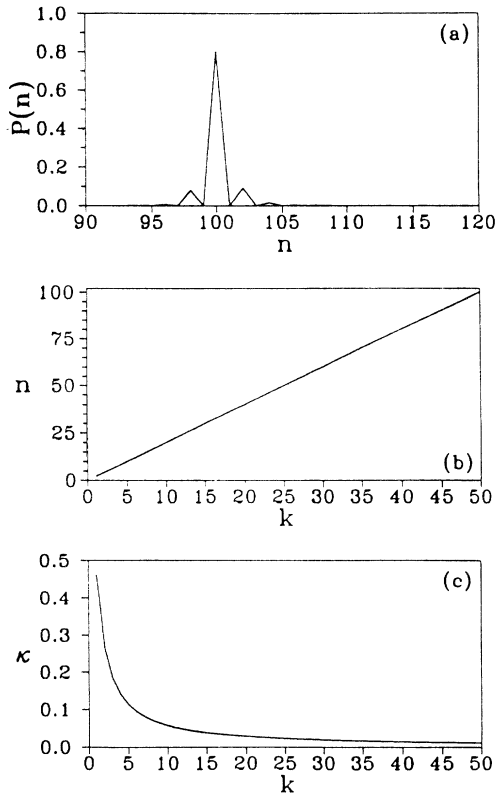

FIG. 5. Same as Fig. 3, but the initial field is described by a squeezed vacuum, with $r=\frac{1}{2}$.

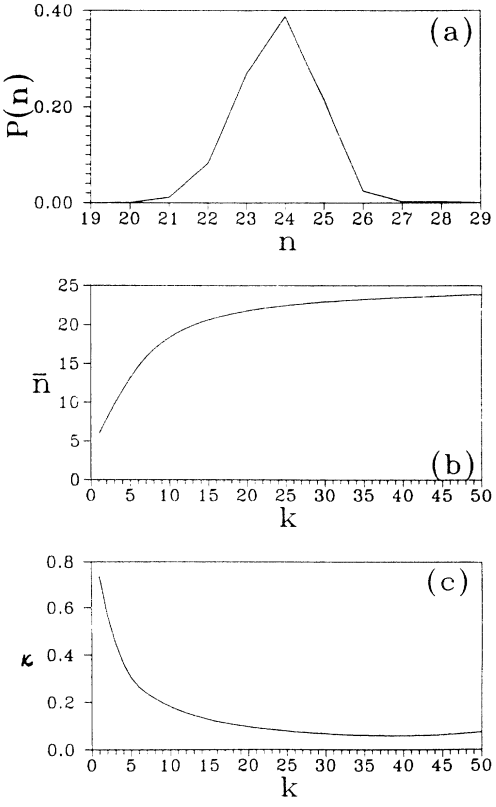

FIG. 7. Same as Fig. 6, but we choose a detuning that balances the effective detuning produced by the Stark-shift parameter, i.e., $\Delta=2$ (in units of λ).

(at $t \cong t_R$), but now $\chi = \frac{1}{2}$ (in units of λ) and $\Delta = 0$. It shows the same behavior as Fig. 3, but the amplification is less strong [see Fig. 6(b)] and the shape of the photon distribution is distorted [see Fig. 6(a)]. In Fig. 7 we obtain the same effects, but now we are balancing the effective detuning given by the Stark parameter with a detuning $\Delta = 2$ (in units of λ).

So far we have imagined each atom to interact with the field for an identical and special time t_R. This time choice is crucial and we show that some effects are not present if each atom interacts for the same time, but which differs from t_R. In Fig. 8(a), we have chosen $t_I = \pi/2\lambda$, half the revival time $\Delta = \chi = 0$, and plot the PD for an initial coherent state $|\alpha|^2 = 4$. We still note oscillations in the PD, but, even though there is linear amplification, [see Fig. 8(b)] the width of the distribution now increases, so that the sub-Poissonian factor [Fig. 8(c)] κ is around 1 (the case for a coherent state), almost as if a linear displacement operator represented the atomic pumping.

B. Total field density matrix

We derive in this subsection the total field density matrix, in order to use it to study the dynamics in phase space and the purity of the field. From Eq. (2.11), we obtain for the modified field reduced density matrix after one atom has interacted with the field,

$$\rho_{nm}^{(1)} = \langle n | \rho_F(t) | m \rangle ,$$
$$= A_n A_m d_n^{*(0)} d_m^{(0)} + B_n B_m d_{n-2}^{*(0)} d_{m-2}^{(0)} , \quad (3.4)$$

where the A's and B's are given in Eq. (2.13) and the d's define the initial field statistics. The corresponding field reduced density matrix after k atoms have interacted with the cavity field in succession is given by

$$\rho_{nm}^{(k)} = A_n A_m d_n^{*(k-1)} d_m^{(k-1)} + B_n B_m d_{n-2}^{*(k-1)} d_{m-2}^{(k-1)} . \quad (3.5)$$

From Eq. (3.5) we compute the Husimi quasiprobability Q function as

$$Q^{(k)}(\beta) = \frac{1}{\pi} \langle \beta | \rho^{(k)} | \beta \rangle . \quad (3.6)$$

In Fig. 9 we plot $Q^{(k)}(\beta)$ in phase space, with the axes given by the real and imaginary parts of the complex amplitude $\beta = X + iY$, for an initial coherent state ($|\alpha|^2 = 4$) after 50 atoms have passed through the cavity. The Q function consists of a main peak which is centered around $X \cong 10$, $Y \cong 0$ and which agrees with the amplification shown in Fig. 3. It has a shape that resembles a "banana state," because, as the field is being amplified and distorted from its initial state to a much more sub-Poissonian state, the phase-space distribution evolves from an initial Gaussian by a deformation into an annular structure more characteristic of a number state. Of course, it only approaches a number state asymptotically, as it retains its original number uncertainty.

We use Eq. (3.5) to compute the parity parameter $\zeta = 1 - \mathrm{Tr}_F(\rho_F^2)$. The field starts in a pure state, so ζ is zero, but become entangled with the atomic states so that the purity parameter is expected in general to increase. This parameter is plotted in Fig. 10 for $\Delta = \chi = 0$, where we note that basically the atom and the field disentangle

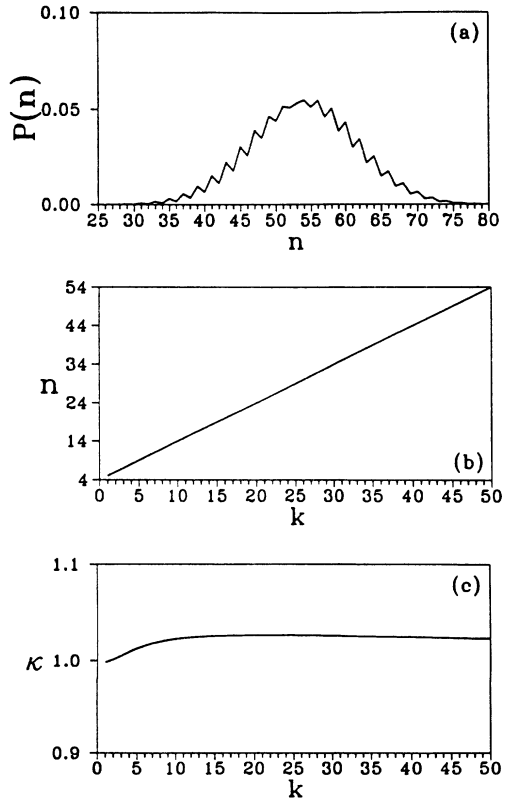

FIG. 8. Same as Fig. 3, but each atom interacts for a time $t = t_R/2$ with the cavity field.

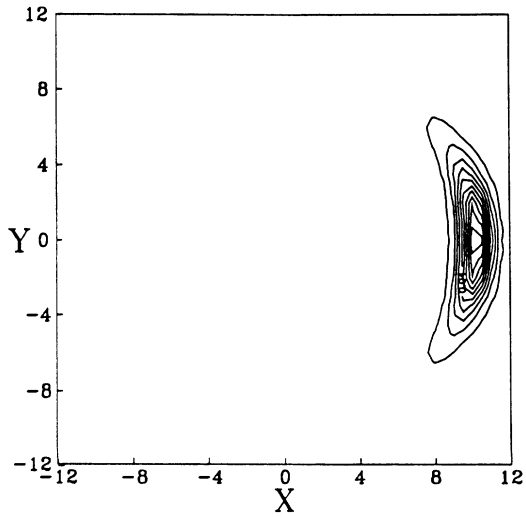

FIG. 9. Field quasiprobability Q function after 50 atoms have passed through the cavity, initially in a coherent state with $|\alpha|^2 = 4$. Atoms enter the cavity in their excited states, and the interaction time $t = t_R$.

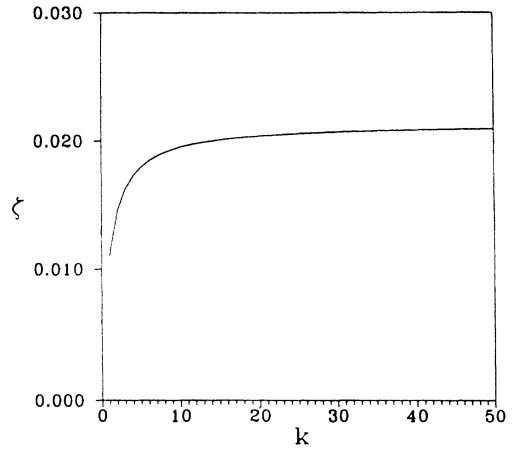

FIG. 10. Purity parameter ζ after 50 atoms have passed through the cavity, initially in a coherent state with $|\alpha|^2=4$. Atoms enter the cavity in their excited states, and the interaction time $t=t_R$.

after each interaction. Although the purity slowly decreases (i.e., ζ slowly increases) with increasing atomic number, it remains very small. This process is, for instance, a much purer one than that obtained from the one-photon Jaynes-Cummings model [16,18] in the middle of the collapse region where it is known that an asymptotically disentangled state is generated. We shall make use of the fact that atoms leave the cavity almost in their pure state in Sec. III C, where we derive an analytical solution for the problem.

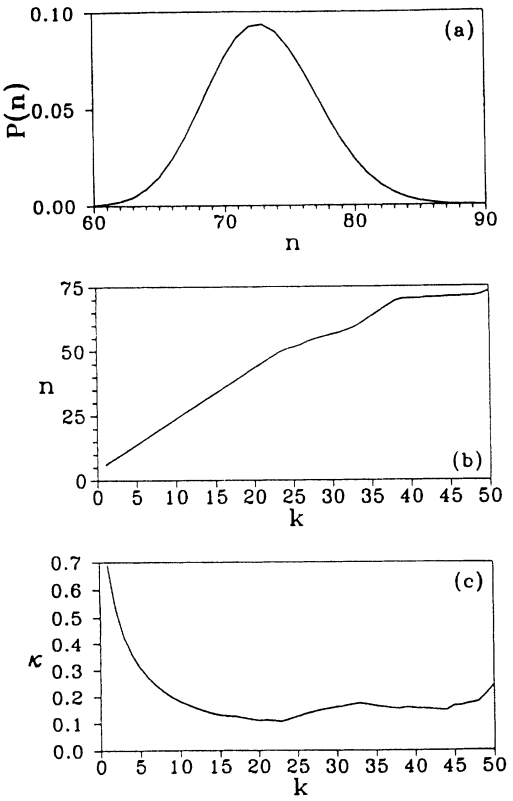

FIG. 11. Same as Fig. 3, but we arrange for the atoms to interact the cavity field with a set of interaction times chosen at random from a Gaussian distribution modeling beam flight times. The width of the Gaussian distribution is $t_R/100$, and it is centered at t_R.

C. Different interaction times

We now study the behavior of the cavity field, when the time of flight is different for each atom corresponding, for example, to the case of a beam of atoms with a distribution of velocities exciting the cavity. From Eq. (2.11) we get the PD after k atoms have passed through the cavity, atom "1," interacting for a time t_1, atom "2" for a time t_2, etc.

$$P_n^{(k)}(t_1,t_2,\ldots,t_k)=A_n^2(t_k)P_n^{(k-1)}(t_{k-1}) +B_n^2(t_k)P_{n-2}^{(k-1)}(t_{k-1})\ . \quad (3.7)$$

In Fig. 11(a) we plot the PD when atoms interact with the cavity field with a distribution of times picked at random from a Gaussian probability, which one might expect from a velocity-selected atomic beam. The initial field state is a coherent state ($|\alpha|^2=4$ and $\chi=\Delta=0$). The width of the Gaussian distribution of interaction times is $t_R/100$ and is centered on t_R. We note that although the amplification is not as strong as in the case of constant interaction times, the shape is still preserved. The amplification is reduced because, as the number of photons in the cavity increases, there are more Rabi oscillations in the atomic inversion and, then, for a small deviation of the interaction time, the probability of the atom exiting the cavity in the ground state decreases, giving less energy to the field. In Fig. 11(b), we plot the average number of photons where we have a good amplification, and in Fig. 11(c), we plot the sub-Poissonian parameter κ, which shows sub-Poissonian photon statistics.

IV. CONCLUSIONS

We have shown in this paper that by interacting atoms with cavity fields via two-photon resonant transitions and for especially chosen interaction times (the revival time), amplified and strongly sub-Poissonian (Fock state) fields can be generated. Because of the behavior of the atomic inversion, which oscillates around zero, so that each atom on average deposits a single photon to the field, we have linear amplification of the average photon number for most of the interaction times we choose (t_R, $t_R/2$, etc.). We have derived approximate expressions for the two-photon atomic inversion for coherent and even coherent fields.

ACKNOWLEDGMENTS

We would like to thank S. M. Barnett, B. M. Garraway, and G. M. Palma for useful discussions. This work was supported in part by the Mexican Consejo Nacional de Ciencia y Tecnología (CONACyt), the U. K. Science and Engineering Research Council, the Rothschild Foundation, and by the Royal Society.

[1] P. Filipowicz, J. Javanainen, and P. Meystre, J. Opt. Soc. Am. B **3**, 906 (1986); Phys. Rev. A **34**, 3077 (1986); J. J. Slosser, P. Meystre, and S. L. Braunstein, Phys. Rev. Lett. **63**, 934 (1989). For a review of micromaser theory, see P. Meystre, *Progress in Optics,* edited by E. Wolf (Elsevier, New York, 1992), p. 263. For experimental work on one-photon micromasers, see G. Rempe, H. Walther, and N. Klein, Phys. Rev. Lett. **58**, 353 (1987); D. Meschede, H. Walther, and G. Müller, *ibid.* **54**, 551 (1985); G. Rempe, W. Schleich, M. O. Scully, and H. Walther, in *Proceedings of the 3rd International Symposium on the Foundation of Quantum Mechanics* (Physical Society of Japan, Tokyo, 1989), pp. 294. The underlying Jaynes-Cummings model is reviewed by B. W. Shore and P. L. Knight, J. Mod. Opt. **40**, 1195 (1993).

[2] J. Krause, M. O. Scully, and H. Walther, Phys. Rev. A **36**, 4547 (1987).

[3] M. Brune, J. M. Raimond, P. Goy, L. Davidovich, and S. Haroche, Phys. Rev. Lett. **59**, 1899 (1987).

[4] B. M. Garraway, B. Sherman, H. Moya-Cessa, P. L. Knight, and G. Kurizki, Phys. Rev. A **49**, 535 (1994); see also K. Vogel, V. M. Akulin, and W. P. Schleich, Phys. Rev. Lett. **71**, 1816 (1993).

[5] A. Rosenhouse-Dantsker (unpublished).

[6] M. Brune, J. M. Raimond, and S. Haroche, Phys. Rev. A **35**, 154 (1987); L. Davidovich, J. M. Raimond, M. Brune, and S. Haroche, *ibid.* **36**, 3771 (1987); M. Orszag and J. C. Retamal, Opt. Commun. **79**, 455 (1990); M. Orszag. L. Roa, and R. Ramírez *ibid.* **86**, 147 (1991); M. Orszag, R. Ramírez, J. C. Retamal, and L. Roa, Phys. Rev. A **45**, 6717 (1992); S. Qamar, K. Zaheer, and M. S. Zubairy, Opt. Commun. **78**, 341 (1990).

[7] S. J. D. Phoenix and P. L. Knight, J. Opt. Soc. Am. B **7**, 116 (1990).

[8] H. Moya-Cessa, V. Buzek, and P. L. Knight, Opt. Commun. **85**, 267 (1991).

[9] P. L. Knight and B. Shore, Phys. Rev. A **48**, 642 (1993).

[10] S. Stenholm, Phys. Rep. C **6**, 1 (1973).

[11] V. Buzek, A. Vidiella-Barranco, and P. L. Knight, Phys. Rev. A **45**, 6570 (1992); see also W. Schleich, M. Pernigo, and Fam le Kien, *ibid.* **44**, 2174 (1991).

[12] A. Vidiella-Barranco, H. Moya-Cessa, and V. Buzek, J. Mod. Opt. **39**, 1441 (1992).

[13] R. Loudon and P. L. Knight, in a special issue of J. Mod. Opt. **34**, 709 (1987); H. P. Yuen, Phys. Rev. A **13**, 2226 (1976).

[14] J. Eiselt and H. Risken, Phys. Rev. A **43**, 346 (1991).

[15] L. Mandel, Opt. Lett. **4**, 205 (1979).

[16] J. Gea-Banacloche, Phys. Rev. Lett. **65**, 3385 (1990); Phys. Rev. A **44**, 5913 (1991).

[17] Cao Chang-qui and Ding Xiao-hong, Phys. Rev. A **46**, 6042 (1992).

[18] V. Buzek, H. Moya-Cessa, P. L. Knight, and S. J. D. Phoenix, Phys. Rev. A **45**, 8190 (1992).